



Response to a twist in systems with Z_p symmetry: The two-dimensional p -state clock model

Yuta Kumano,¹ Koji Hukushima,² Yusuke Tomita,³ and Masaki Oshikawa¹

¹*Institute for Solid State Physics, University of Tokyo, Kashiwa 277-8581, Japan*

²*Department of Basic Science, University of Tokyo, Tokyo 153-8902, Japan*

³*College of Engineering, Shibaura Institute of Technology, Saitama 337-8570, Japan*

(Received 31 January 2013; revised manuscript received 11 September 2013; published 30 September 2013)

We study response to a twist in the two-dimensional p -state clock model, which has the discrete Z_p symmetry. The response is measured in terms of helicity modulus, which is usually defined with respect to an infinitesimal twist. However, we demonstrate that such a definition is inappropriate for the clock model. The helicity modulus must be defined with respect to a finite, quantized twist which matches the discrete Z_p symmetry of the model. Numerical study of the appropriately defined helicity modulus resolves controversy over the clock model, showing the existence of two Berezinskii-Kosterlitz-Thouless transitions for $p > 4$.

DOI: [10.1103/PhysRevB.88.104427](https://doi.org/10.1103/PhysRevB.88.104427)

PACS number(s): 64.60.De, 05.50.+q, 75.10.Hk

I. INTRODUCTION

Symmetries govern various phases of matter and transitions among them. There are two distinct classes of symmetries: continuous and discrete, with quite different consequences. For example, gapless Nambu-Goldstone modes are required in a spontaneous symmetry breaking phase, only if the symmetry is continuous. The cyclic group Z_p symmetry appears in many important problems of current interest, including the melting transition in the hard-disk model,¹⁻³ antiferromagnetic Ising model/Ising-spin Kondo model on a triangular lattice,⁴⁻⁷ and antiferromagnets in the vicinity of the deconfined quantum-critical point.⁸ While the Z_p symmetry is discrete for any value of p , it approaches to the continuous $U(1)$ symmetry in the limit of $p \rightarrow \infty$. It is an interesting problem if a statistical system with the discrete Z_p symmetry can effectively possess a continuous $U(1)$ symmetry for a large enough p .

Such an emergence of the $U(1)$ symmetry due to statistical fluctuations is indeed predicted in the framework of the renormalization group (RG). The emergent $U(1)$ symmetry is expected, in two dimensions, for sufficiently large p in a finite region of the phase diagram. Namely, the now-standard RG analysis⁹ shows that systems with the Z_p symmetry have, for $p > 4$, a Berezinskii-Kosterlitz-Thouless (BKT) phase^{10,11} between two BKT transitions. The BKT transition at higher temperature is similar to that in the XY model with the $U(1)$ symmetry. It can be said that the $U(1)$ symmetry emerges in the models with only the Z_p symmetry.

However, we may ask if the discrete nature of the Z_p symmetry of the microscopic model is actually negligible at the BKT transition with the emergent $U(1)$ symmetry. In this paper, we address this question by analyzing the response of Z_p symmetric systems to a twist. We demonstrate that, in measuring the response of the system to the twist, the discrete symmetry at the microscopic level has to be respected despite the emergent continuous symmetry in the macroscopic scale. Namely, the helicity modulus, which is usually defined with respect to an infinitesimal twist, must be rather defined with respect to a finite, quantized twist which matches the discrete Z_p symmetry of the model. This crucial fact has been apparently overlooked, resulting in the popular use of the inappropriately defined helicity modulus for models with the Z_p symmetry.^{12,13} We elucidate these points, by analyz-

ing a concrete example, the two-dimensional p -state clock model.

This paper is organized as follows: In the next section, we introduce the two-dimensional p -state clock model with respect to a twist and briefly review preceding studies of the model. Section III is devoted to an analysis of the helicity modulus by high-temperature expansion. In Sec. IV, we show numerical studies of the appropriately defined helicity modulus. In the last section, we give conclusions which support the existence of two BKT transitions for $p > 4$.

II. MODEL

We consider the p -state clock model on the two-dimensional $L \times L$ square lattice with periodic boundary conditions:

$$H_p = - \sum_{\langle \vec{r}, \vec{r}' \rangle} \cos(\theta_{\vec{r}} - \theta_{\vec{r}'} - A_{\vec{r}, \vec{r}'}), \quad (1)$$

where $\vec{r} = (r_1, r_2)$ ($r_{1,2} \in \mathbb{Z}, 0 \leq r_{1,2} < L$), $\langle \vec{r}, \vec{r}' \rangle$ runs over all the nearest neighbor sites on the square lattice, and $0 \leq \theta_{\vec{r}} < 2\pi$ takes integral multiples of $2\pi/p$. We have set the coupling constant to unity. The gauge field $A_{\vec{r}, \vec{r}'}$ is usually set to zero but is introduced to impose a twist, as we will discuss later.

According to the seminal RG analysis,⁹ for $p \leq 4$, there is a single critical point separating disordered and ordered phases, while the BKT phase appears for $p > 4$ in a finite range of temperature between the disordered and ordered phases. This has been also supported by later examinations.¹⁴⁻¹⁶ In order to verify the prediction numerically, one needs a good physical quantity measurable in numerical simulations. In the systems with the $U(1)$ symmetry, although the BKT phase exhibits no spontaneous symmetry breaking, it is characterized by the response to a twist. The helicity modulus,¹⁷ which quantifies such a response, is finite in the BKT phase while it vanishes in the high-temperature (disordered) phase. At the BKT transition separating these two phases, the helicity modulus exhibits a universal jump,¹⁸ which was confirmed numerically and experimentally.^{19,20}

The standard RG picture on the Z_p symmetric models seems to suggest, for $p > 4$, the similar behavior of the helicity modulus at the BKT transition between the high-temperature disordered phase and the BKT phase. However, several recent

numerical studies^{12,13,21,22} do not conform to this expectation. While details differ in each work, they suggest, in particular, the absence of the BKT transition for $p = 5$. The most important evidence against the BKT transition picture is the lack of the universal jump of the helicity modulus at the transition. It would be a major problem for statistical physics if the standard RG picture turns out to be incorrect. On the other hand, Monte Carlo simulations are very effective for the clock model and the numerical results also must be taken seriously.

III. DEFINITION OF HELICITY MODULUS FOR SYSTEMS WITH DISCRETE SYMMETRY

The helicity modulus is often defined with respect to an infinitesimal global twist. We first introduce the gauge field $A_{\vec{r}+\hat{x},\vec{r}} = \tilde{\Delta}/L$ for all the sites \vec{r} , where $\hat{x} = (1,0)$ is the unit vector in the x direction, as a global twist to the Hamiltonian (1). Then we define the helicity modulus by the second derivative,

$$\tilde{\Upsilon}_p \equiv \left. \frac{\partial^2 F_p(\tilde{\Delta})}{\partial \tilde{\Delta}^2} \right|_{\tilde{\Delta}=0}, \quad (2)$$

where $F_p(\tilde{\Delta})$ is the free energy in the presence of the twist $\tilde{\Delta}$ introduced above. Being defined in terms of the derivative, it probes the response to an infinitesimal twist spread over the entire system.

This definition of the helicity modulus is convenient for numerical calculations, since it can be written as an expectation value of a local physical quantity,

$$\tilde{\Upsilon}_p = \frac{1}{L^2} \left\langle \sum_{\vec{r}} \cos \phi_{\vec{r}+\hat{x},\vec{r}} \right\rangle - \frac{\beta}{L^2} \left\langle \left(\sum_{\vec{r}} \sin \phi_{\vec{r}+\hat{x},\vec{r}} \right)^2 \right\rangle, \quad (3)$$

where $\beta = 1/T$ is the inverse temperature (we normalize the Boltzmann constant to unity), and $\phi_{\vec{r}+\hat{x},\vec{r}} \equiv \theta_{\vec{r}+\hat{x}} - \theta_{\vec{r}}$.

It was indeed this definition of the helicity modulus that was used in Refs. 12 and 13 to study the p -state clock model. The most striking aspect of their results for $p = 5$ is that the helicity modulus thus obtained does not show the universal jump which is expected for a BKT transition. In fact, the helicity modulus is nonvanishing even in the high-temperature disordered phase, in stark contrast to the expected behavior at a BKT transition.

This seems to contradict with the standard RG picture with two BKT transitions.⁹ In the standard picture, the helicity modulus should vanish in the disordered phase, while it diverges proportionally to the system size L in the ordered phase owing to the extra free energy of the induced domain wall. However, we find that $\tilde{\Upsilon}_p$ remaining nonzero in the high-temperature phase is rather a consequence of the inappropriate definition of the helicity modulus. Indeed, for any finite p , we shall demonstrate that the helicity modulus as defined in Eq. (2) is nonvanishing at an arbitrary high temperature, where the system is certainly disordered, even in the thermodynamic limit.

To see this, let us consider the high-temperature (character) expansion of Eq. (2), using the identity $e^{\beta \cos \phi} = \sum_{k=-\infty}^{\infty} I_k(\beta) e^{ik\phi}$ for the modified Bessel function I_k . For the

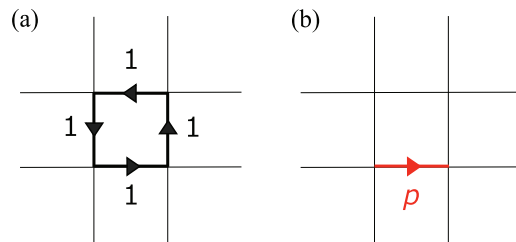


FIG. 1. (Color online) (a) A lowest order diagram for the XY model. This diagram has no contribution to $\tilde{\Upsilon}_p$. (b) A lowest order diagram which has a nonzero contribution to $\tilde{\Upsilon}_p$ for the p -state clock model.

XY model with the $U(1)$ symmetry, we find

$$\tilde{\Upsilon} = \frac{1}{\beta L^2} \sum_{\substack{\{k_{\vec{r},\vec{r}'} \in \mathbb{Z}\} \\ \sum_{\vec{r}'} k_{\vec{r},\vec{r}'} = 0}} \left(\sum_{\vec{r}} k_{\vec{r},\vec{r}+\hat{x}} \right)^2 \prod_{\langle \vec{r},\vec{r}' \rangle} \frac{I_{k_{\vec{r},\vec{r}'}}(\beta)}{I_0(\beta)}, \quad (4)$$

where $k_{\vec{r},\vec{r}'}$ is an integer defined for each link between the nearest neighbor pairs, and $k_{\vec{r},\vec{r}'} \equiv -k_{\vec{r}',\vec{r}}$. The constraint $\sum_{\vec{r}'} k_{\vec{r},\vec{r}'} = 0$ means that the lattice divergence vanishes at every site. Thus, each term in the high-temperature expansion corresponds to a configuration of an integer-valued “flux field” $\{k_{\vec{r},\vec{r}'}\}$ forming closed loops. Since $I_k(\beta) \sim \beta^{|k|}$, each term corresponds to the order $\sum_{\langle \vec{r},\vec{r}' \rangle} |k_{\vec{r},\vec{r}'}|$ of the high-temperature expansion. In Fig. 1(a), we show the lowest-order nontrivial diagram in the high-temperature expansion for the XY model. Unless there is a flux loop winding the entire system, which can occur only above the order L , we have $\sum_{\vec{r}} k_{\vec{r},\vec{r}+\hat{x}} = 0$. Thus, for the XY model in the thermodynamic limit $L \rightarrow \infty$, the helicity modulus defined in Eq. (2) vanishes at any finite order in the high-temperature expansion (4).

Now let us consider the p -state clock model. The only difference from the XY model is due to the fact that $\sum_{\theta=0,2\pi/p,\dots,2\pi(p-1)/p} e^{in\theta} = p$, if n is an integral multiple of p . Thus, the high-temperature expansion of Eq. (2) for the p -state clock model is exactly the same as Eq. (4), except for the constraint at each site now replaced by $\sum_{\vec{r}'} k_{\vec{r},\vec{r}'} \equiv 0 \pmod{p}$. This allows various flux configurations which were not permitted in the XY model. The lowest order in the high-temperature expansion among such configurations is given by $k_{\vec{R},\vec{R}+\hat{x}} = p$ for a certain site \vec{R} and all other fluxes $k_{\vec{r},\vec{r}'} = 0$. In Fig. 1(b), we show the corresponding diagram for the p -state clock model. This term leads to a nonvanishing contribution to $\tilde{\Upsilon}_p$ as

$$\tilde{\Upsilon}_p \sim \frac{p}{(p-1)!} \left(\frac{\beta}{2} \right)^{p-1}, \quad (5)$$

in the lowest order of β . This proves that the helicity modulus $\tilde{\Upsilon}_p$ as defined in Eq. (2) does not vanish at an arbitrary high temperature, for any finite p , even in the thermodynamic limit. This implies that Eq. (2) does not sharply distinguish the disordered and other phases. We note that, while this is the case actually for an arbitrary large finite p , the contribution becomes rapidly smaller for larger p . This is the reason why the problem in the high-temperature phase has been noticed numerically only for smaller p , in particular $p = 5$.

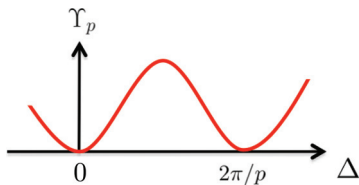


FIG. 2. (Color online) Twist dependence of the helicity modulus Υ_p for the p -state clock model in disordered phase. Υ_p is zero if the twist angle Δ is an integral multiple of $2\pi/p$. The finiteness of Υ_p with respect to an infinitesimal twist reflects the curvature at $\Delta = 0$ of the free energy difference, $F_p(\Delta) - F_p(0)$, in Eq. (6).

Thus we need a different quantity to describe the phase transition. Intuitively, the problem with the infinitesimal twist we have used could be understood as the introduction of a mismatch between neighboring spins, whose directions are quantized in the p -state clock model. Therefore, let us define the helicity modulus as a response to the finite twist $A_{\vec{r}+\hat{x},\vec{r}} = \Delta$ localized on the horizontal links localized on a single column $\vec{r} \in \mathcal{C} \equiv \{(L-1, r_2) | 0 \leq r_2 < L\}$:

$$\Upsilon_p \equiv \frac{2(F_p(\Delta) - F_p(0))}{\Delta^2}. \quad (6)$$

Matching with the Z_p symmetry of the model would require Δ to be an integral multiple of $2\pi/p$. We note that, in the original introduction of the helicity modulus,¹⁷ the twist was not restricted to be infinitesimal.

In the high-temperature expansion, the difference between $Z_p(\Delta)$ and $Z_p(0)$ comes only from the factor $\exp[i\Delta \sum_{\vec{r} \in \mathcal{C}} k_{\vec{r},\vec{r}+\hat{x}}]$. Thus, if Δ is an integral multiple of $2\pi/p$, the effect of the twist in the p -state clock model again disappears, even under the relaxed constraint $\sum_{\vec{r}} k_{\vec{r},\vec{r}+\hat{x}} \equiv 0 \pmod{p}$, at any finite order of the high-temperature expansion in the thermodynamic limit. $\Upsilon(2\pi/p)$ indeed vanishes exactly in the high-temperature disordered phase, as physically required for the helicity modulus. The vanishing of the helicity modulus in the high-temperature expansion was pointed out in a related context in Ref. 23. To illustrate the point, we show the twist dependence of the helicity modulus $\Upsilon_p(\Delta)$ in the disordered phase (in the thermodynamic limit) schematically in Fig. 2. $\Upsilon_p(\Delta)$ is zero only when the twist angle Δ is an integral multiple of $2\pi/p$. The popularly used helicity modulus $\tilde{\Upsilon}_p$ defined with respect to an infinitesimal twist does not vanish even in the disordered phase, reflecting the curvature at $\Delta = 0$ of the free energy difference, $F_p(\Delta) - F_p(0)$, in Eq. (6). In contrast to the clock model, in the XY model with the continuous $U(1)$ symmetry, the helicity modulus $\Upsilon_p(\Delta)$ vanishes for an arbitrary twist.

This is an explicit example in which the difference between the discrete and the continuous symmetries at the microscopic level appears in the macroscopic physical quantity, even when the systems belong to the same phase. Again, we emphasize that, for the response to a twist to distinguish different phases, it should vanish in the disordered phase. This means that we should apply a finite twist which matches the discrete Z_p symmetry of the model, in order to distinguish phases properly.

IV. NUMERICAL CALCULATIONS OF THE FREE ENERGY DIFFERENCE DUE TO A TWIST

We have concluded that, in order to distinguish different phases of the clock model in terms of its response to a twist, the twist angle must be an integral multiple of $2\pi/p$. The change in the free energy due to a twist of a finite angle cannot be simply reduced to an expectation value of a local physical quantity, unlike in the case of the infinitesimal twist. Thus it is more difficult to calculate the response in Monte Carlo simulations. Nevertheless, it is possible to do so, as discussed in the following.

We need to obtain the ratio of the partition functions, $Z_p(\Delta)/Z_p(0)$, which can be calculated by boundary-flip Monte Carlo method.^{24,25} This method treats not only spins but also boundary conditions as variables. This is realized by introduction of a boundary condition variable $\sigma = \{0, 1\}$ with a twist $A_{\vec{r}+\hat{x},\vec{r}} = \sigma \Delta$ localized on the horizontal links on a single column $\vec{r} \in \mathcal{C} \equiv \{(L-1, r_2) | 0 \leq r_2 < L\}$ to the Hamiltonian (1). $\sigma = 0$ (1) corresponds to a periodic (twisted) boundary condition, respectively. The ratio of partition functions $Z_p(\Delta)/Z_p(0)$ can be estimated from the ratio of expectation values of each boundary condition $\langle \delta_{\sigma,1} \rangle / \langle \delta_{\sigma,0} \rangle$.

We update both spins and the boundary condition variable σ , by the Metropolis algorithm. To overcome the critical slowing down of spin variables, we use the Wolff cluster method²⁶ at low temperatures. In contrast, it is difficult to update the boundary condition at low temperatures because the free energy difference between the periodic and twisted boundary conditions is rather large in the BKT and ordered phase. To overcome this difficulty, we add another term, $g\sigma$, in Hamiltonian (1) to balance the free energy difference between the two boundary conditions. The parameter g is also updated during the simulation adaptively to achieve the balance, in order to minimize the rejection rate. In our simulations, the number of Monte Carlo steps are $O(10^7)$ up to $O(10^9)$ after equilibration.

Here we focus on the case with $p > 4$, where the standard RG picture predicts two BKT transitions while some of the recent numerical studies found apparent contradictions with it. We emphasize that, while those recent papers do agree with the RG picture and identify BKT transitions for sufficiently large p , the helicity modulus as defined in Eq. (2) $\tilde{\Upsilon}_p$ they studied is nonzero at an arbitrary high temperature. It is just that Eq. (2) is smaller for higher values of p and more difficult to be detected numerically. We still need to verify if the alternative quantity Υ_p , defined with respect to a finite twist in Eq. (6), indeed confirms the BKT transitions. We show the temperature dependence of Υ_p for $p = 5$ and 6, in Figs. 3(a) and 3(b). In the low-temperature regime, colored blue, Υ_p increases proportionally to the system size L , while it decreases towards zero in the high-temperature regime, colored beige. These are precisely the expected behaviors in the low-temperature ordered (spontaneously symmetry breaking) and the high-temperature disordered phases. These behaviors of Υ_p are indeed what are expected for the helicity modulus and successfully distinguish the three phases. In contrast, the helicity modulus $\tilde{\Upsilon}_p$ in Figs. 3(c) and 3(d), defined as Eq. (2) with respect to the infinitesimal twist, does not exhibit physically expected behaviors for a helicity modulus. While the disagreement of Eq. (2) with the standard RG picture

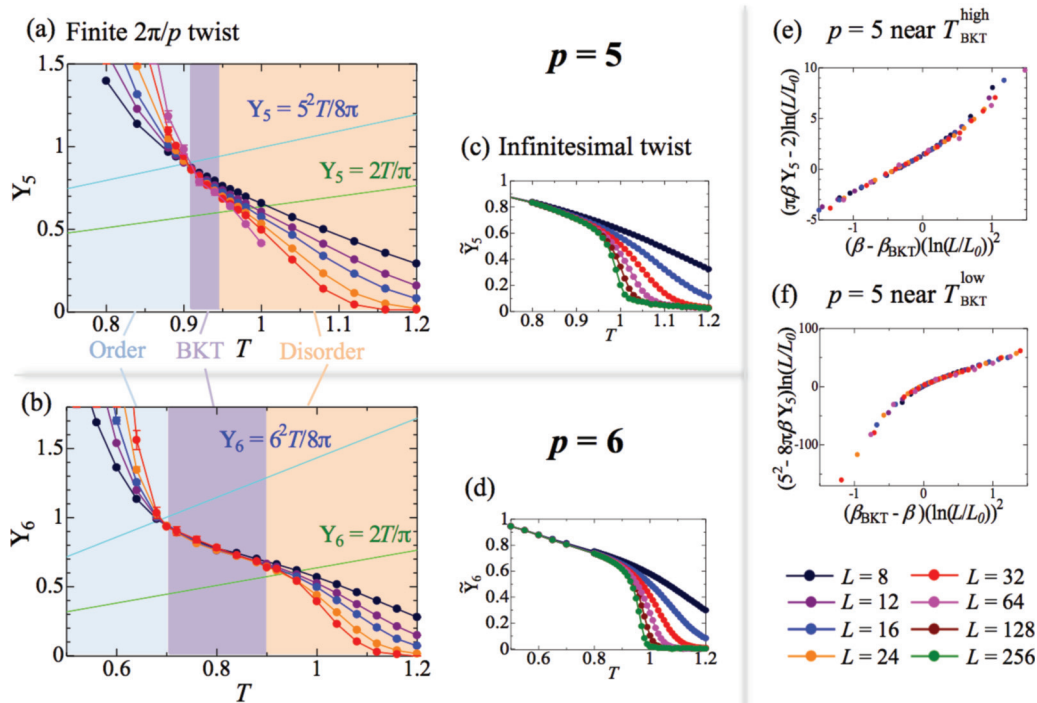


FIG. 3. (Color online) (a)–(d) Temperature dependence of Υ_p and $\tilde{\Upsilon}_p$ for $p = 5$ and $p = 6$. In both cases, $\tilde{\Upsilon}_p$ with respect to an infinitesimal twist does not reflect each phase appropriately. In comparison, for Υ_p with respect to the finite twist $2\pi/p$, we can find three regions: blue, purple, and beige regions correspond to ordered, BKT, and disordered phase, respectively. In addition, as L is increased, Υ_p approaches the universal value on the higher and lower transition points, with the universal relations (7) and (8) shown, respectively, by yellow-green and aqua lines. Colored lines are for a guide to the eyes. (e) and (f) Finite-size scaling of Υ_5 near $T_{\text{BKT}}^{\text{high}}$ and $T_{\text{BKT}}^{\text{low}}$. All the data points collapse into universal curves in both cases. The estimated scaling parameters are $(T_{\text{BKT}}, L_0) = (0.944, 0.8), (0.908, 1.9)$ for (e) and (f), respectively.

in the high-temperature phase, especially for $p = 5$, was discussed previously, we also emphasize that Eq. (2) does not detect the low-temperature ordered phase. The “finite twist” helicity modulus Υ_p we have introduced does distinguish the three phases, as is physically expected.

Moreover, in the intermediate temperature regime (purple), Υ_p tends to be independent of L , which is indeed the expected behavior in the BKT phase.¹⁷ This is rather clear for $p = 6$; the approximate transition temperatures estimated from Fig. 3(b) for $p = 6$, $T_{\text{BKT}}^{\text{high}} \sim 0.90$ and $T_{\text{BKT}}^{\text{low}} \sim 0.70$, are in agreement with the estimates $T_{\text{BKT}}^{\text{high}} \sim 0.90008(6)$ and $T_{\text{BKT}}^{\text{low}} \sim 0.7014(11)$ obtained by a different method.²⁷ On the other hand, the existence of the BKT phase for $p = 5$ is not very clear in Fig. 3(a) because of the finite-size effects.

The well-known consequence of the BKT transition picture is the “universal jump” of the helicity modulus. In terms of RG, it is a consequence of the fact that the BKT transition occurs at a definite Gaussian coupling constant (also known as “Luttinger parameter” or “compactification radius”) where the leading perturbation becomes marginal. A similar argument also can be applied to the transition at the low-temperature side of the BKT phase.⁹ For $p > 4$, we obtain the universal relations at the two transitions as

$$\lim_{T \rightarrow T_{\text{BKT}}^{\text{high}} - 0} \Upsilon_p = \frac{2}{\pi} T_{\text{BKT}}^{\text{high}}, \quad (7)$$

$$\lim_{T \rightarrow T_{\text{BKT}}^{\text{low}} + 0} \Upsilon_p = \frac{p^2}{8\pi} T_{\text{BKT}}^{\text{low}}. \quad (8)$$

In Figs. 3(a) and 3(b), we compare the temperature dependence of the “finite twist” helicity modulus Υ_p with the universal relations (7) and (8) shown, respectively, by yellow-green and aqua lines. We can find, as L is increased, Υ_p approaches the universal values on the higher and lower transition points. They do not, however, completely converge owing to finite-size effects.

Therefore, we have also performed a finite-size scaling analysis based on the RG theory at each transition. In the vicinity of the transition at higher temperature, $T_{\text{BKT}}^{\text{high}}$, the Z_p anisotropy y_p is always irrelevant, so we can approximately neglect y_p to obtain the standard BKT RG equations for the vortex fugacity y and the Gaussian coupling,^{9,14} The scaling form of the helicity modulus was derived²⁸ from the RG equations as

$$x(T, L) = l^{-1} f(l^2 \delta), \quad (9)$$

where $x = \pi\beta\Upsilon_p - 2$, $\delta = \beta - \beta_{\text{BKT}}^{\text{high}}$ and $l = \ln(L/L_0)$. Here, $\beta_{\text{BKT}}^{\text{high}} = 1/T_{\text{BKT}}^{\text{high}}$ is the inverse transition temperature, and L_0 is a scaling parameter. They are the fitting parameters to the data. On the other hand, near the transition at the lower temperature, $T_{\text{BKT}}^{\text{low}}$, the vortex fugacity y is always irrelevant and thus may be neglected. The RG equations involving y_p , in the vicinity of the lower-temperature transition, $T_{\text{BKT}}^{\text{low}}$, are similar to that for the higher-temperature transition at $T_{\text{BKT}}^{\text{high}}$. As a consequence, for the lower-temperature transition at $T_{\text{BKT}}^{\text{low}}$, a similar analysis in the vicinity of the lower-temperature transition $T_{\text{BKT}}^{\text{low}}$ leads

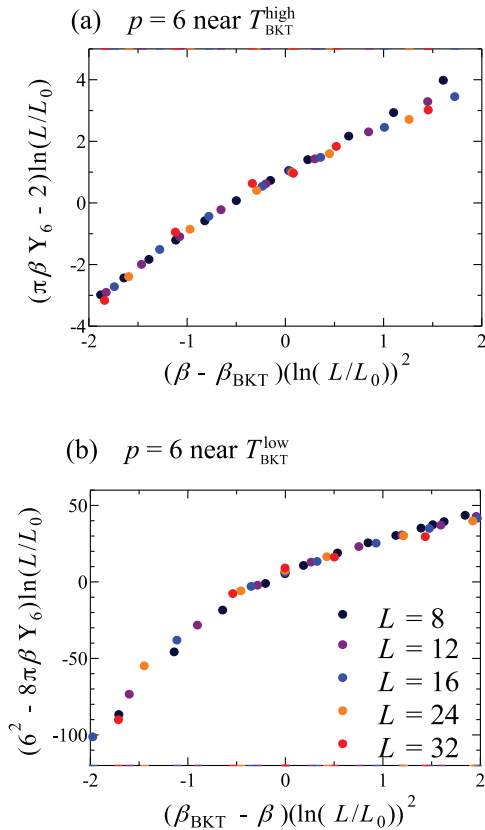


FIG. 4. (Color online) (a) and (b) Finite-size scaling of Υ_6 near $T_{\text{BKT}}^{\text{high}}$ and $T_{\text{BKT}}^{\text{low}}$. All the data points collapse into universal curves in both cases. The estimated scaling parameters are $(T_{\text{BKT}}, L_0) = (0.904, 0.5), (0.700, 0.9)$ for (a) and (b), respectively.

to the scaling equation, $x'(T, L) = l^{-1} f'(l^2 \delta')$, where $x' = p^2 - 8\pi\beta\Upsilon_p$ and $\delta' = \beta_{\text{BKT}}^{\text{low}} - \beta$, respectively, where $\beta_{\text{BKT}}^{\text{low}} = 1/T_{\text{BKT}}^{\text{low}}$, and f' is a different scaling function from f . The present scaling analysis is more sophisticated and reliable than the direct measurement of the universal jump of the helicity modulus, which is often used in literature.

In Figs. 3(e) and 3(f), we show the finite-size scaling of Υ_5 near each of the transitions, at $T_{\text{BKT}}^{\text{high}}$ and $T_{\text{BKT}}^{\text{low}}$. We can find all the data points collapse into universal functions if we set two scaling parameters as $(T_{\text{BKT}}, L_0) = (0.944, 0.8), (0.908, 1.9)$, respectively. These are in good agreement with $T_{\text{BKT}}^{\text{high}} = 0.95147(9)$ and $T_{\text{BKT}}^{\text{low}} = 0.90514(9)$ estimated earlier by a different numerical method.²⁹

We have also confirmed, for $p = 6$, that Υ_6 obeys the same BKT finite-size scaling at each transition point. In Figs. 4(a) and 4(b), we show the finite-size scaling of Υ_6 near each of the transitions, at $T_{\text{BKT}}^{\text{high}}$ and $T_{\text{BKT}}^{\text{low}}$. The estimated

transition temperatures $T_{\text{BKT}}^{\text{high}} = 0.904(5)$ and $T_{\text{BKT}}^{\text{low}} = 0.700(4)$ from the finite-size scaling are in good agreement with $T_{\text{BKT}}^{\text{high}} = 0.90008(6)$ and $T_{\text{BKT}}^{\text{low}} = 0.7014(11)$ determined earlier by a different numerical method.²⁷

V. CONCLUSIONS AND DISCUSSIONS

All our observations support, for $p > 4$, the existence of the BKT phase separated by two BKT transitions from the high-temperature disordered phase and from the low-temperature ordered phase, as predicted by RG.⁹ Much of the apparent contradiction with recent numerical results was rather due to the ‘‘helicity modulus’’ adopted in the numerical studies, which was defined with respect to an infinitesimal twist. Such a quantity is inappropriate for the p -state clock model with the discrete Z_p symmetry.

Thus we have established that, for this model, the helicity modulus instead has to be defined with respect to a finite quantized twist which matches the Z_p symmetry of the system. Namely, in measuring the response to a twist, the discrete nature of the Z_p symmetry at the microscopic level has to be respected, even when the continuous $U(1)$ symmetry emerges. Although we have restricted the analysis to the simple p -state clock model in the present paper, our discussion can be readily applied to more general models with Z_p symmetry, including the XY model with a perturbation which breaks the $U(1)$ symmetry down to Z_p . The present result would also have implications in a wider range of problems with discrete symmetries or discretized degrees of freedom.

Note added. After the submission of the present paper (see also³⁰), Baek, Mäkelä, Minnhagen, and Kim³¹ analyzed the p -state clock model using the helicity modulus with respect to a finite twist, as introduced in the present paper. Their conclusion for $p = 5$ is, however, different from ours.

ACKNOWLEDGMENTS

We would like to thank Naoki Kawashima for valuable suggestions and fruitful discussions. The present work is supported in part by Grant-in-Aid for Scientific Research (KAKENHI) for Priority Areas No. 20102008 from MEXT of Japan, and by US National Science Foundation Grant No. NSF PHY11-25915 while Y.K. and M.O. performed a part of the present work at Kavli Institute for Theoretical Physics, UC Santa Barbara. Y.K. was partially supported by an Advanced Leading Graduate Course for Photon Science (ALPS) grant. A part of numerical calculations for this work was done at Supercomputer Center, Institute for Solid State Physics, University of Tokyo.

¹B. I. Halperin and D. R. Nelson, *Phys. Rev. Lett.* **41**, 121 (1978).

²A. P. Young, *Phys. Rev. B* **19**, 1855 (1979).

³H. Watanabe, S. Yukawa, Y. Ozeki, and N. Ito, *Phys. Rev. E* **69**, 045103 (2004).

⁴M. Mekata, *J. Phys. Soc. Jpn.* **42**, 76 (1977).

⁵D. P. Landau, *Phys. Rev. B* **27**, 5604 (1983).

⁶S. Fujiki, K. Shutoh, and S. Katsura, *J. Phys. Soc. Jpn.* **53**, 1371 (1984).

⁷H. Ishizuka and Y. Motome, *Phys. Rev. Lett.* **108**, 257205 (2012).

⁸T. Senthil, A. Vishwanath, L. Balents, S. Sachdev, and M. P. A. Fisher, *Science* **303**, 1490 (2004).

- ⁹J. V. Jose, L. P. Kadanoff, S. Kirkpatrick, and D. R. Nelson, *Phys. Rev. B* **16**, 1217 (1977).
- ¹⁰V. L. Berezinskii, *Sov. Phys. JETP* **32**, 493 (1971).
- ¹¹J. M. Kosterlitz and D. J. Thouless, *J. Phys. C* **6**, 1181 (1973).
- ¹²S. K. Baek and P. Minnhagen, *Phys. Rev. E* **82**, 031102 (2010).
- ¹³C. M. Lapilli, P. Pfeifer, and C. Wexler, *Phys. Rev. Lett.* **96**, 140603 (2006).
- ¹⁴S. Elitzur, R. B. Pearson, and J. Shigemitsu, *Phys. Rev. D* **19**, 3698 (1979).
- ¹⁵K. Nomura, *J. Phys. A* **39**, 2953 (2006).
- ¹⁶G. Ortiz, E. Cobanera, and Z. Nussinov, *Nucl. Phys. B* **854**, 780 (2012).
- ¹⁷M. E. Fisher, M. N. Barber, and D. Jasnow, *Phys. Rev. A* **8**, 1111 (1973).
- ¹⁸D. R. Nelson and J. M. Kosterlitz, *Phys. Rev. Lett.* **39**, 1201 (1977).
- ¹⁹P. Minnhagen and B. J. Kim, *Phys. Rev. B* **67**, 172509 (2003).
- ²⁰D. J. Bishop and J. D. Reppy, *Phys. Rev. Lett.* **40**, 1727 (1978).
- ²¹C.-O. Hwang, *Phys. Rev. E* **80**, 042103 (2009).
- ²²S. K. Baek, P. Minnhagen, and B. J. Kim, *Phys. Rev. E* **81**, 063101 (2010).
- ²³T. Kanazawa, *Ann. Phys.* **324**, 1634 (2009).
- ²⁴A. P. Gottlob and M. Hasenbusch, *J. Stat. Phys.* **77**, 919 (1994).
- ²⁵K. Hukushima, *Phys. Rev. E* **60**, 3606 (1999).
- ²⁶U. Wolff, *Phys. Rev. Lett.* **62**, 361 (1989).
- ²⁷Y. Tomita and Y. Okabe, *Phys. Rev. B* **65**, 184405 (2002).
- ²⁸K. Harada and N. Kawashima, *Phys. Rev. B* **55**, R11949 (1997).
- ²⁹O. Borisenko, G. Cortese, R. Fiore, M. Gravina, and A. Papa, *Phys. Rev. E* **83**, 041120 (2011).
- ³⁰Y. Kumano, K. Hukushima, Y. Tomita, and M. Oshikawa, arXiv:1301.6166.
- ³¹S. K. Baek, H. Mäkelä, P. Minnhagen, and B. J. Kim, *Phys. Rev. E* **88**, 012125 (2013); arXiv:1307.5512.